

A SMART SURVEILLANCE SYSTEM FOR HUMAN FALL-DOWN DETECTION USING DUAL HETEROGENEOUS CAMERAS

Shaou-Gang Miaou, Cheng-Yu Chien, Fu-Chiau Shih

Multimedia Computing and Telecommunications Laboratory, Department of Electronic Engineering, Chung Yuan Christian University, Chung-Li, 32023 Taiwan, R.O.C.

Chia-Yuan Huang

Industrial Technology Research Institute, Hsinchu, 310 Taiwan, R.O.C.

Keywords: Surveillance system, omni-directional camera, PTZ camera, fall detecting.

Abstract: We propose a new surveillance system that uses both omni-directional (OD) and Pan/Tilt/Zoom (PTZ) cameras with heterogeneous characteristics and a relatively simple image processing algorithm to achieve the goal of real time surveillance. The system is demonstrated for detecting the occurrence of human's fall-down event. An OD camera has a 360° viewing angle. It is used here to replace the multiple traditional cameras having limited viewing angles in order to reduce the system cost. A PTZ camera is also used in the system to track the target of interest and verify the occurrence of the event. Various unique features obtained from OD images are used for fall down detection and a multi-classifier approach is used for better recognition performance. Experimental results show that the system is quite robust to sudden changes of walking paths and different directions of falling. During the tracking process, a moving target is captured and its representative coordinates is obtained based on the processing of continuous OD images. The coordinates of the target in the OD camera space will be converted to its corresponding three dimensional (3D) coordinates in a real-world space. This derived information is served as guidance for the automatic control of the PTZ camera to track the moving target as closely as it can. By combining the advantages of two heterogeneous types of cameras, our experimental results show that the proposed system can track the moving target well without the need of a complicated method, showing the feasibility and potential of the system.

1 INTRODUCTION

With the rapid development of technology and medical treatment, the average life span of human increases. As a result, the percentage of the population group with age 65 or more becomes higher and higher in many parts of the world. The number of the elderly with chronic disease, melancholia, and psychosis is increasing as well. The elderly suffer from the fall accidents more than young people according to the statistics. A fall accident not only causes physical injury but also produces emotional disturbance for the elderly.

More and more elderly need long-term care (Chen, 2002). However, there may not be enough manpower to take care so many elderly. One way to

alleviate the seriousness of this manpower shortage problem is to deploy a surveillance system for the detection of fall down events and other dangerous situations.

A traditional camera usually has a fixed viewing angle that limits the possible coverage of surveillance in an environment. Multiple cameras are usually needed to cover the entire surrounding of the environment. A Pan/Tilt/Zoom (PTZ) camera can extend its viewing angles by constantly panning and tilting the camera with a motor-controlled mechanism. However, this is not very practical for long-term surveillance because of the considerable waste of power and the quick wearing of motor-driven mechanical parts. Besides, the event of interest may not be observed if the scanning cycle of

the PTZ camera is much longer than the duration of the event. Another way to extend the viewing angle of a tradition camera is to put it on a moving carrier. Although it can increase the cruising range of a surveillance area, the area covered by the camera at a time instant is still limited. And there may be some dead spots left un-attended.

To solve the problems mentioned above, Greiffenhagen et al. developed a new surveillance system based on the use of an omni-directional (OD) camera which basically consists of a traditional camera and a convex mirror such that it has a 360° viewing angle at any time instant (Greiffenhagen, 2001). After the OD camera was proposed, many applications were developed based on the use of the camera. For example, with the images taken by the OD camera, Mituyosi et al. tried to capture and track the features of a human face (eyes, mouths, etc) (Mituyosi, 2003).

Although an OD camera can capture the image from every angle at one shot, the resulting image is distorted due to the use of the convex mirror. Normally, the distortion level increases as it moves from the center of the image to the border of the image. In order to cover large surveillance areas with reasonably good image quality, Morita used several OD cameras and a computer network system to connect them (Morita, 2003). Similarly, Lee also used multiple OD cameras for outdoor surveillance (Lee, 2002).

Again, the distortion from the convex mirror in a PTZ camera could cause a serious problem for some applications but it does have the advantage of the broadest viewing angle. Thus, we use a PTZ camera to replace the possible use of the second or more OD cameras in our surveillance system. These two heterogeneous types of cameras can be operated in a complementary manner. We use an OD camera for the preliminary tracking of a moving object in the OD space and if the moving object presents the features of interest, the system automatically controls the PTZ camera to capture a sequence of the undistorted and clear images that contain the moving object for further visual inspection (by naked eyes). Several advantages are associated with the system that has such dual but heterogeneous cameras. First, one OD camera can cover large enough surveillance area with little dead spots. Second, the pan, tilt, and zoom capability of the PTZ camera is fully exploited to get clear visual information of the moving object for better visual assessment. Third, the moving object may be locked and stayed in locked by a PTZ

camera much more easily if the object's location information obtained from the OD images is available. This dual camera system can be used in many long-term and smart surveillance applications. In this paper, we demonstrate its use in the detection of human falling event in an indoor environment, such as living room or sanatorium. Once a true falling event is identified, emergency care may be activated immediately to save lives. In this application, we use an OD camera to detect the falling event. If a suspicious event is detected by the system, an alarm and/or message as well as PTZ images will be sent to designated person who will verify the event based on the PTZ images by naked eyes. This will eliminate unnecessary false alarms and enhance the reliability and credibility of the system.

In the following sections, we will discuss the issues of moving object extraction, fall-down event recognition, and moving object tracking. The experimental results and conclusion will be given in the last two sections, respectively.

2 SYSTEM FRAMEWORK AND FLOWCHART

We use the system framework shown in Figure 1. First, we use an OD camera to capture the image of the whole scene in a surveillance area. The resulting OD images will be used to detect the existence of a moving object. If a moving object is identified, its representative coordinates on the OD image plane will be converted to the real-world coordinates in a three-dimensional (3D) space. The coordinate information in 3D can be used to control a PTZ camera such that the moving object can be tracked and locked by the PTZ camera easily. The images taken by the PTZ camera will be sent back to an intended user of the surveillance system via some network links for further visual inspection and verification.

The system flowchart on signal processing tasks is shown in Figure 2. Here, we use only simple and basic image processing methods to capture a moving object. Once the moving object is detected, we do the coordinate conversion and fall detecting. If a suspicious fall-down event is detected, PTZ images will be sent to intended users to verify the event and see if it is a true event or just a false alarm.

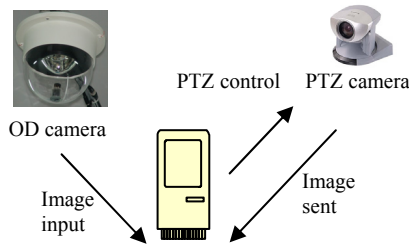


Figure 1: System framework.

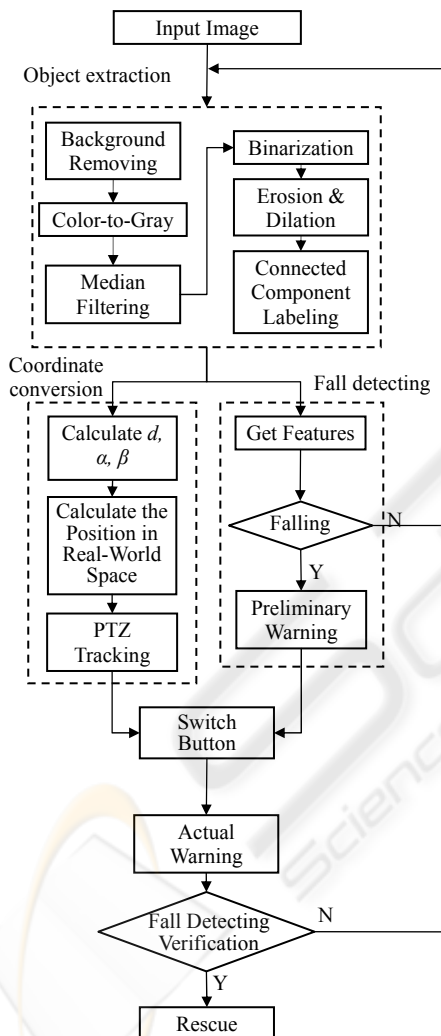


Figure 2: System flowchart.

2.1 Object Capturing

The moving object detecting approach that we use here is the background subtraction method which is simple and well-known. As usual, background is

updated on a regular basis in order to overcome the problem of light intensity change and/or chromatism. We use Equation (1) to capture a foreground image.

$$D(x,y) = |f_c(x,y) - f_b(x,y)| \quad (1)$$

where $f_c(x,y)$ denotes the pixel intensity at location (x,y) of input image, $f_b(x,y)$ represents the pixel intensity of background image at the same location, and $D(x,y)$ denotes a difference image. Then we use Equation (2) to eliminate the potential noise and shadows and get a binarized image:

$$\hat{D}(x,y) = \begin{cases} 255, & \text{if } D(x,y) > T \\ 0, & \text{else} \end{cases} \quad (2)$$

where T is an empirical threshold. When $D(x,y) > T$, the system considers that a pixel at location (x,y) is a potential pixel of the foreground image; otherwise, it could be just part of noises or shadows that need to be removed. Then we use some techniques in morphology to capture a complete foreground image. Finally, we use the well-known connected component labeling method to identify the moving object. Figure 3 shows an original image and a foreground image after performing the image processing tasks discussed above.

After the object of interest is captured, we use two sub-systems for further processing. One is the fall detecting sub-system, and the other one is the object tracking sub-system.



Figure 3: The results of foreground image capturing. (a) An original image; (b) A binarized image after noise removal and connected component labeling.

2.2 Fall Detecting Sub-System

2.2.1 Method

When a falling event occurs, the human body usually has significant movement. Thus, we define body line of human body next and use the features associated with the body line for fall-down recognition later. Figure 4 shows the two scanning

methods to find the body line. One is horizontal scanning, and the other is vertical scanning. In Figure 4, the ellipse is used to represent the foreground and the rectangle is used to represent the smallest bounding box that encloses the foreground. All we need is the human body, so each scan line is Δd pixels away from its closest sideline to avoid the inclusion of head and feet parts. The $a_1, a_2, b_1,$ and b_2 are the intersecting points at which the scan lines and the boundary of the foreground object intersect. In addition, Points S and T are the midpoints for a_1 and $a_2,$ and for b_1 and $b_2,$ respectively. Finally, \overline{ST} segment is the potential body line. Figure 4 shows the results of horizontal scans and vertical scans, resulting in two body lines, and we choose the longer one as our final body line. We need both horizontal and vertical scans instead of one of them in order to avoid the situation of wrong body line selection when the major axis of the ellipse is parallel to the x-axis or y-axis.

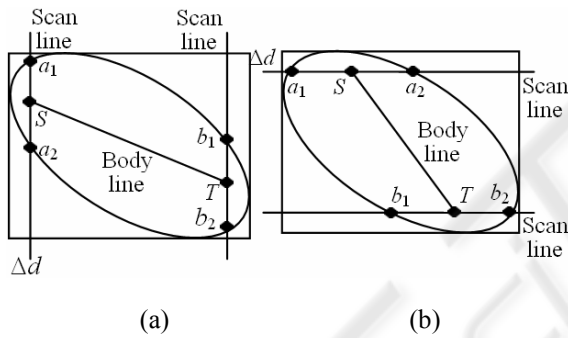


Figure 4: Finding a body line segment. (a) Vertical scanning; (b) Horizontal scanning.

After the body line segment is found, we rename the end points of the segment and call them I and J according to the following rule: The end point closer to the center M (where the OD camera is located) is called I and the other end point is called J , as shown in Figure 5. Next, we define a body line vector \overline{IJ} and a reference line vector \overline{MI} as follows:

$$\overline{MI} = \overline{OI} - \overline{OM} \quad (3)$$

$$\overline{IJ} = \overline{OJ} - \overline{OI} \quad (4)$$

where O is the origin located at the top left corner of the image. The angle θ between these two vectors is defined as

$$\theta = \cos^{-1}(\overline{MI} \cdot \overline{IJ} / \|\overline{MI}\| \|\overline{IJ}\|) \quad (5)$$

where $\overline{MI} \cdot \overline{IJ}$ is the inner product of the vectors \overline{MI} and \overline{IJ} , and $\|\cdot\|$ denotes the norm operation. Figure 6 shows a typical body line vector and a reference line vector imposed on a real-world OD image.

Next, we define the features used for the recognition of fall down event:

- (1) The angle θ defined in Equation (5).
- (2) The length L of body line vector \overline{IJ} .
- (3) The x coordinate of the midpoint of body line.
- (4) The y coordinate of the midpoint of body line.
- (5) The ratio ρ between the length and the width of the rectangle shown in Figure 4.

One set of these five features can be obtained for one image frame. Multiple sets of features can be obtained for the multiple frames contained in an observing window. Let K be the number of frames in the observing window. Then this sliding window is moved such that any two adjacent windows contain $K - 1$ identical image frames and one different frame. In this study, we set K to be 15.

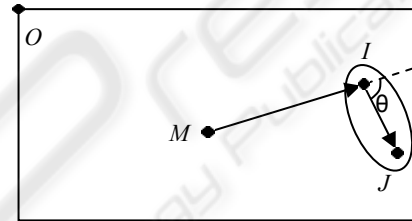


Figure 5: A pictorial representation of body line and reference line vectors.



Figure 6: A typical OD image imposed by body line and reference line vectors and a bounding box (rectangle).

Figure 7 shows the recognition flowchart of the proposed system. Here, a two-stage multiple classifiers is designed to classify the feature vectors from the feature values discussed above. The first (stage) classifier attempts to classify three classes: normal (do not fall), falling down in non-radial direction, and suspicious fall-down in radial direction. If the last class is determined by the first classifier, then the system uses a second (stage) classifier to reduce the false alarm rate. The second classifier is based on the Back-Propagation Neural Network (BPNN).

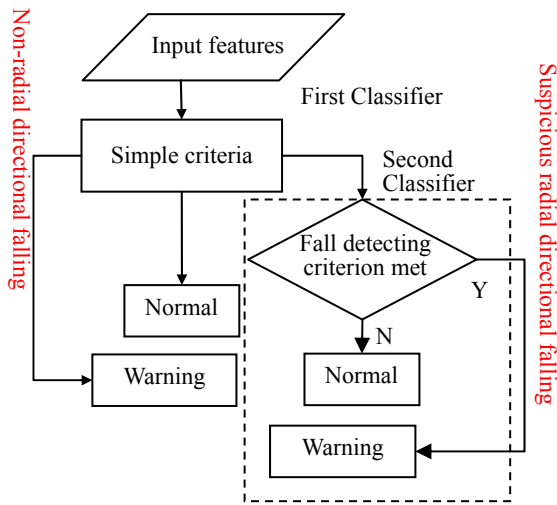


Figure 7: System flowchart of our multiple classifiers.

2.2.2 First Classifier – Simple Decision Criteria

We found that the angle feature defined in Equation (5) does not change much when a target is walking in a normal way or standing according to our experiment. Furthermore, a large angle variation occurs when the fall-down in non-radial direction happens. The simple decision criteria below are used to determine whether the non-radial directional falling occurs.

(1) The average of angle feature values is higher than a preset threshold (indicating the target may be falling).

(2) The displacement of body line midpoint is lower than another preset threshold (indicating the target ceases moving).

If both conditions above are met, the system determines that a non-radial directional fall-down event occurs. However, we can not get a high enough angle variation for radial-direction fall-down, as shown in Figure 8. Thus, we need new recognition features and decision criteria for this situation. We found that when the target falls in radial direction, the length of body line vector changes significantly in some observing windows. Thus, we define two other decision criteria with different features below to deal with this situation:

(1) The variance estimate of body line lengths is higher than a preset threshold.

(2) The displacement of body line midpoint is lower than another preset threshold.

We also found that the body movements for

sitting and squatting also satisfy the two conditions above. Thus, if the two conditions above are met, we can only claim that we have a suspicious case of radial-direction fall-down. Further differentiation between radial-direction fall-down and sitting or squatting is necessary. This is the objective of the second classifier discussed next.

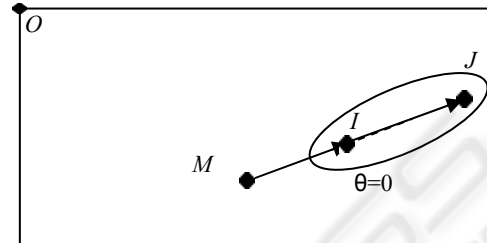


Figure 8: Body line vector and reference vector almost align with each other in radial-direction fall-down.

2.2.3 Second Classifier and Multiple Classifiers

We observed that at least 15 frames are required to complete the process of sitting, squatting, and radial-direction falling. Thus, the system monitors 15 continuous frames and record five parameter values. These five parameters correspond to the five features defined in Section 2.2.1:

- (1) The angle θ defined in Equation (5);
- (2) ΔL : The difference of the length L obtained from two adjacent frames;
- (3) Δx : The displacement in X direction for the x coordinates obtained from two adjacent frames;
- (4) Δy : The displacement in Y direction for the y coordinates obtained from two adjacent frames;
- (5) $\Delta \rho$: The variation between the two ratios ρ obtained from the bounding boxes in two adjacent frames. For each frame in the observing window, these five parameter values are obtained. For 15 consecutive frames, we have a total of 75 parameter values which become the input to the BPNN for training and testing.

2.3 Object Tracking Sub-System

Once an object is obtained, a critical point is defined as the object point that is closest to the center of OD image. The coordinates of this critical point in the OD space will be converted to the real-world 3D coordinates that could be useful for the guidance control of PTZ cameras. Because the image taken by an OD camera is projected from real-word space (as

shown in Figure 9), it is possible to find the corresponding point in real-world space for a point in the OD space. In other words, we need to find the point mapping from OD space to real-world space.

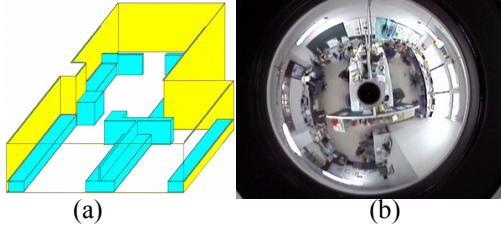


Figure 9: Two different coordinate spaces. (a) A real-world 3D space; (b) Image taken by an OD camera in the OD space.

We know that a point Q' in the real-world space as shown in Figure 9(a) can be projected to the CCD sensor in an OD camera through the reflex of the convex mirror, resulting in the corresponding point Q in the OD space as shown in Fig. 9(b). This idea is further illustrated in Figure 10. After we capture the critical point in the OD image [marked by \odot in Figure 11(a)], we can calculate some useful parameter values as follows:

$$d = \sqrt{Q_x^2 + Q_y^2} \quad (6)$$

$$\alpha = \tan^{-1}\left(\frac{Q_y}{Q_x}\right) \quad (7)$$

where d represents the distance between the critical point to the center of OD image and α is the angle of that point with respect to the x -axis, as shown in Figure 11.

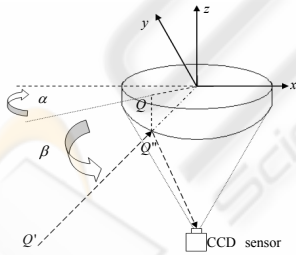


Figure 10: Imaging principle of an OD camera (Yu, 1999).

In addition, the coordinates of Q' can be derived as

$$Q' = \left[\frac{m \cos \alpha}{\tan \beta}, \frac{m \sin \alpha}{\tan \beta}, -m \right] \quad (8)$$

where m denotes a known constant, representing the vertical distance (or height) from the floor to the OD camera, and β denotes the vertical angle of the

critical point with respect to the x - y plane in Figure 10.

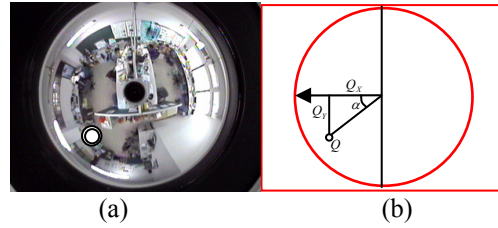


Figure 11: Position of a critical point in OD space. (a) an OD image; (b) parameter calculated from the OD image information.

We can find the corresponding position of the critical point in real-world space by Equation (8) but we still need one more value for the parameters other than the d and α calculated previously. Specifically, we need to find the value for the parameter $\tan \beta$. However, it can not be obtained directly from OD images. In fact, we need to estimate it and one way to do so is as follows. First, design an n -point line array pattern as shown in Figure 12. Then, we attempt to find the position mapping between the points in the OD image and their corresponding points in real-world space. As shown in Figure 12, we have

$$\tan \beta_i = \frac{h_i}{l} \quad (9)$$

$$k_i = \frac{d_i}{r} \quad (10)$$

where β_i denotes the angle β for Point i (or P_i), h_i represents the vertical distance between the plane x - y in real-world space and Point i (or P_i), l is the horizontal distance between the line in the array pattern and the center of the OD camera in real-world space, d_i is the distance from Point i to the OD image center in OD space, r is the radius of the largest circle containing meaningful image data in OD images, and k_i is a known ratio for Point i . Numerical values of these parameters are shown in Table 1 (only one third is shown). Given these data set, we use a MATLAB curve fitting tool to calculate the best relationship curve between $\tan \beta$ and k . The result is in Equation (11):

$$\tan \beta = 9.929 \times e^{\left(\frac{k-0.158}{0.226}\right)^2} + 2.068 \times e^{\left(\frac{k-0.0442}{0.6032}\right)^2} \quad (11)$$

Therefore, given the radius r and the distance d , we get k from Equation (10) and then obtain the value for $\tan \beta$ from Equation (11). Finally, we get the converted coordinates in real-world space by using Equation (8).

After we get an estimate for the coordinates of

the critical point in real-world space, we can send proper commands to the PTZ camera via RS232 port by properly setting panning, tilting, and zooming such that the moving target can be centered in the resulting PTZ images with appropriate size. For a new critical point detected, the PTZ camera may need a different set of commands to control it properly. Continue in this way, the moving object can be tracked effectively.

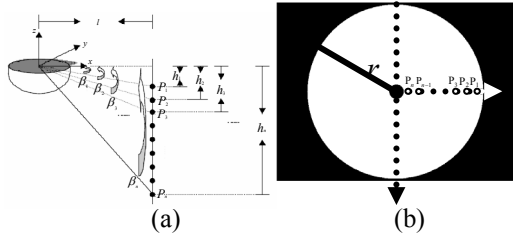


Figure 12: Experiment trying to find the relationship between two coordinate spaces (Hsu, 2004). (a) Data points in real-world space; (b) data points after projection.

Table 1: Relationship between $\tan \beta$ and k .

i	l (mm)	h (mm)	$\tan \beta_i$	k_i	d (pixel)	r (pixel)
1	135	33.0	0.24	0.90	104	116
2		36.0	0.27	0.88	102	
3		41.0	0.30	0.86	100	
4		47.0	0.35	0.84	97	
5		57.5	0.43	0.80	93	
6		68.0	0.50	0.76	88	
7		84.2	0.62	0.72	83	
8		100.5	0.74	0.66	76	
9		122.0	0.90	0.59	69	
10		143.0	1.06	0.52	60	
11		170.0	1.26	0.47	54	
12		197.0	1.46	0.41	47	
13		229.0	1.70	0.36	42	
14		261.0	1.93	0.32	37	
15		298.5	2.21	0.28	33	

3 RESULTS AND DISCUSSION

3.1 Fall Detecting

Figure 13 shows a possible value variation for Feature (5) and Feature (1) given in Section 2.2.1. It is found that the values for ratio features may change significantly in both walking and falling, while the values of angel feature change significantly only in a falling situation. Thus, the angle feature may be more robust than the ratio feature with respect to different walking paths.

The evaluation criteria we use for the fall

detection sub-system are accuracy, specificity, and Kappa values (Siegel, 1988) (Lee, 2000). Table 2 shows the performance comparison between the results of using a single (first stage) classifier and a multiple classifiers. The multiple-classifier approach always outperforms the single classifier method. This demonstrates the effectiveness of the second stage classifier in the sub-system.

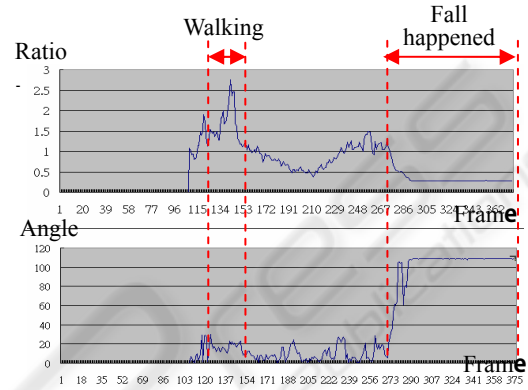


Figure 13: A comparison between ratio and angle features.

Table 2: Performance comparison between single classifier approach and multiple-classifier approach.

	Accuracy	Specificity	Kappa
Simple criterion	0.82	0.72	0.64
Multiple classifier	0.87	0.88	0.73

3.2 Real-Time Tracking

We give a simple experiment to evaluate the precision of the tracking sub-system. A target is asked to walk along a specified path. Then the system predicts the walking path based on the information from OD images and the coordinate conversion formula given in Equation (8). The result shows that the predicted walking path is quite close to the actual walking path, but some errors exist. The errors may come from image processing (wrong feet or critical point positions are obtained) and the curving fitting formula given in Equation (11) for $\tan \beta$.

We check several fixed and known points to verify the precision of the coordinate conversion formula. Eight points shown in Figure 14 are selected in our experiment. The results are shown in Table 3.

As Table 3 shows, the error could be as high as

10 pixels or more. However, the size of the image considered here is 752*771 and the errors in X-direction and Y-direction are about 0.8% and 0.84%, respectively. Thus, the error is relatively small and thus the formula in Equation (11) is acceptable. We can also see that the errors in the inside block are smaller than those in outside block. The reason is that the input image is distorted more seriously in the outside block than in the inside block. Therefore, we found that bad image processing result (such as wrong feet detecting) is the main source contributing the error and the curve fitting equation has little contribution on inaccuracy.

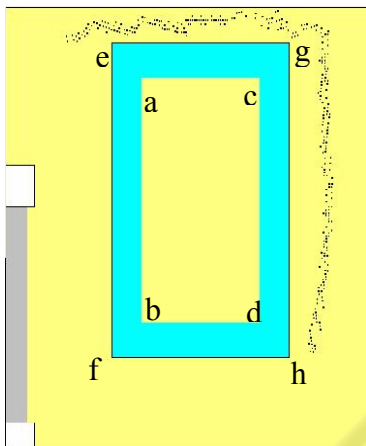


Figure 14: Top-view diagram of experimental environment (Size: 752*771).

Table 3: Errors for coordinate conversion.

Position		X direction		Y direction	
		Error (pixels)	Average error (pixels)	Error (pixels)	Average error (pixels)
Inside	a	0.33	6.03	7.07	5.95
	b	5.30		2.00	
	c	7.23		0.27	
	d	2.99		10.16	
Outside	e	8.38	8.09	1.45	7.02
	f	12.00		16.78	
	g	0.79		9.67	
	h	11.20		0.19	

In Li's work, a PTZ camera must be installed directly under an OD camera and no coordinate conversion is used (Li, 2006). Several drawbacks are associated with the approach proposed by Li. First, the installation constraint may prevent its system from being practical because the installation of the system may not be possible in some environments. Second, the PTZ camera can cover a limited

surveillance area (with only 180° viewing angle). In other words, half of the room can not be seen. Third, the tracking accuracy in Li's approach may be inferior since no coordinate conversion is used for error compensation. In our proposed system, we do not have the installation constraint mentioned above. Theoretically, it can be installed anywhere in the environment. Of course, some locations may be more suitable than others in practical consideration. We conducted two more experiments to further illustrate the problems associated with the approach proposed by Li and demonstrate the advantages with the proposed approach in this paper. One is for the environment where the PTZ camera is installed directly under the OD camera (Point A in Figure 15), and the other is for the environment where the PTZ camera is installed at anywhere except just under the OD camera (Point B in Figure 15). Again, we assign a walking path for a target to follow and compare the prediction accuracy of the path obtained by the two approaches.

In the first experiment, since the PTZ camera is put right under the OD camera, the accuracy results for the approaches are quite similar and are not shown here. In addition, a common drawback of this installation is the limited viewing angle. For example, suppose someone moves from Point B to Point C along the BC segment and the PTZ camera points to the exact south from the center in Figure 15. In this case, half of the BC segment cannot be seen and the tracking can not continue. In the second experiment, we install the PTZ camera at Point B. Note that the approach by Li uses the detected moving target directly from OD images without any correction. So if the target walks along the straight line BC, the line will be distorted and becomes a curve as shown in Figure 15. This curve rather than straight line information is provided to the PTZ camera for tracking. Thus, with this erroneous information, smooth and continuous tracking becomes harder in this case. This drawback will not occur with the proposed approach. Since we have corrected the distortion in some extent, the detected path is roughly a line (as Figure 14 shows). With this more accurate information, the smooth and continuous tracking by the PTZ camera is easier. In summary, the proposed approach has advantages over the one proposed by Li, although additional computation is required.

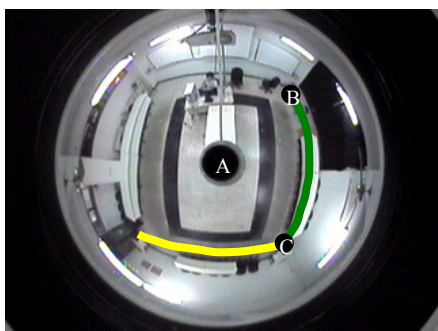


Figure 15: OD image showing an assigned path.

4 CONCLUSIONS

In this paper, a smart surveillance system for human fall-down event detection based on dual heterogeneous cameras is proposed. We attempt to combine the advantages of both OD camera and PTZ camera. Specifically, we can use the wide viewing angle capability provide by the OD camera for preliminary tracking and fall detecting, followed by the use of a PTZ camera for fall detection verification, face detection or other possible applications. The precision for the coordinate conversion between two coordinate spaces is good. The feet detection error in image processing is the main contribution of the inaccuracy. In our system, a PTZ camera can be installed at the best location for surveillance in real-world situation, which can offer installation flexibility and convenience.

ACKNOWLEDGEMENTS

This work is supported in part by the National Science Council of R. O. C. under Contract NSC-95-2221-E-033-069-MY3.

REFERENCES

- Chen, M. S. (2002). *The Empirical Research on the Elderly Living in Nursing Homes --- Illustrated by the Elders the Three Public Nursing Home of Chiayi City*. Master Thesis, NanHua University, Taiwan, R.O.C.
- Greiffenhagen, M., Comaniciu, D., Neimann, H., & Ramesh, V. (2001). Design, Analysis, and Engineering of Video Monitoring Systems: An Approach and A

Case Study, *Proc. of IEEE*, vol. 89, no. 10, pp. 1498-1517.

- Hsu, M. Y. (2004). An Application of the Panoramic Camera to the Positioning and the Path Planning of An Automatic Navigated Vehicle, *The 21th National Conf. on Mechanical Eng., The Chinese Society of Mechanical Eng.* pp.1725-1730, 2004.
- Lee, J. W., You, S., & Neumann, U. (2002). Tracking with Omni-directional Vision for Outdoor AR Systems, *Proc. of the Int. Symp. on Mixed and Augmented Reality*, pp. 47-56.
- Lee, T. W. (2000). *Statistics*, Taipei: Best-Wise Publishing Co., Ltd.
- Li, C. K. (2006). *Using Omni-Directional and PTZ Cameras to Implement Real-Time Tracking of Moving Objects on a DSP Board*, Master Thesis, Dept. of Electronic Eng., Chung-Yuan Christian University, Taiwan, R.O.C.
- Mituyosi, T., Yagi, Y., & Yachida, M. (2003). Real-time Human Feature Acquisition and Human Tracking by Omni-directional Image Sensor, *Proc. of IEEE Conf. on Multisensor Fusion and Integration for Intelligent System*, pp. 258-263.
- Morita, S., Yamazawa, K. & Yokoya, N. (2003). Networked Video Surveillance Using Multiple Omnidirectional Cameras, *Proc. of IEEE Int. Symposium on Comput. Intelligence in Robotics and Automation*, pp. 1245-1250, Kobe, Japan.
- Siegel, S., & Castellan, N. (1988). *Nonparametric Statistics for the Behavioral Sciences, 2nd Ed.* New York: McGraw-Hill.
- Yu, F. P. (1999). *Using Panoramic Video Camera Direct Pan-Tilt-Zoom Cameras*. Master Thesis, National Taiwan University, Taiwan, R.O.C.